Journal of Applied Physics ARTICLE scitation.org/journal/jap

Origins of observational errors in field sweep DC measurements for unidirectional magnetoresistance

Cite as: J. Appl. Phys. **132**, 213907 (2022); doi: 10.1063/5.0127587
Submitted: 22 September 2022 · Accepted: 11 November 2022 ·
Published Online: 2 December 2022

Yihong Fan, Renata Saha, Yifei Yang, and Jian-Ping Wang[a)]

AFFILIATIONS

Electrical and Computer Engineering Department, University of Minnesota, Minneapolis, MN, 55414, USA

[a)]**Author to whom correspondence should be addressed:** jpwang@umn.edu

ABSTRACT

Understanding the mechanisms of unidirectional magnetoresistance (UMR) has become an important topic for its potential application of a two-terminal spin–orbit torque device. Field sweep DC measurements have been proposed and adopted to measure the value of UMR instead of second harmonic measurements. In this paper, potential measurement errors in conventional DC measurements are investigated. Oersted field and field-like torque usually do not influence the measurement, but a large field-like torque was found to lead to an anisotropic magnetoresistance difference when the sample is not perfectly aligned with the external field. The existence of ordinary magnetoresistance was also found to contribute to a large background. In this paper, an alternative measurement method for UMR was proposed and demonstrated to address those issues related to previous DC measurements. Our work may broaden the understanding of the error sources of UMR measurements and provide a reliable DC measurement method for the characterization of UMR.

I. INTRODUCTION

Magnetoresistive behaviors with 360° angular dependence are critical to the reading process in spintronic memory and logic devices. Among these, the unidirectional spin Hall magnetoresistance (USMR)[1–7] has attracted a great deal of attention due to its potential application in two-terminal spintronic devices.[2,7] The conventional model for USMR is the current-in-plane giant magnetoresistance model,[1–4] which treats the spin accumulation at the interface as an effective magnetic layer. The USMR value is proportional to the applied electric field or the current density.[1–4] Therefore, the second harmonic measurement is commonly used to obtain USMR value.[1–6]

Recently, a variety of research efforts has pointed out other contributions to USMR, including spin torque,[8] magnon creation and annihilation,[9–12] and topological interface and structure.[5–7] Among these effects, the spin Hall effect related mechanisms are not the only origin, thus instead of calling these USMR, unidirectional magnetoresistance (UMR) is a more accurate name for such observations. Different origins of UMR lead to a different field- and current-dependent behaviors. As the UMR value may no longer be proportional to the electric field,[3,8] field sweep under DC can be a path to study the UMR effect with contributions other than spin Hall effect origins.[6,8]

However, measuring UMR with DC accurately is challenging because of its small magnitude compared to the large background signal. The dominant signal in DC measurement is the anisotropic magnetoresistance (AMR), which has a period of 180° and magnitudes larger than the UMR signal. Although theoretically, the AMR will stay the same when the field is reversed by 180°, real experiments can always have setup offsets which could result in a difference in the AMR value. The existence of the Oersted field and field-like torque (FLT) can generate this difference when an angular offset exists. The influence of the Oersted field and field-like torque on UMR DC measurement has not been systematically investigated. Besides AMR, ordinary magnetoresistance (OMR) can also serve as a field-dependent background. This work studies the influence of the Oersted field and FLT and discusses the limitation of accuracy in field-dependent DC measurements. The field-dependent UMR curve with an angular offset is obtained through both experiments and theories in Ta/CoFeB bilayer structures, and results show an AMR-originated error term is usually negligible but can be comparable to the UMR signal in the case of a large FLT.

The influence of OMR is also discussed. An angular- and field-dependent method is demonstrated and suggested to obtain a more accurate UMR value. The obtained UMR value in Ta/CFB is consistent with the result from second harmonic measurements.

II. RESULTS AND DISCUSSION

A. Influence of field-like torque and Oersted field on field dependence measurement

We first studied whether the existence of an angular offset of the external field will influence the obtained UMR value. Spin–orbit torque (SOT) contributions are commonly measured by the change of AMR signals via both DC and second harmonic measurements.[13–15] Since the UMR signal is magnitudes smaller than the AMR signal, a small change in the AMR signal by the SOT effect can lead to a contribution to the total UMR signal.

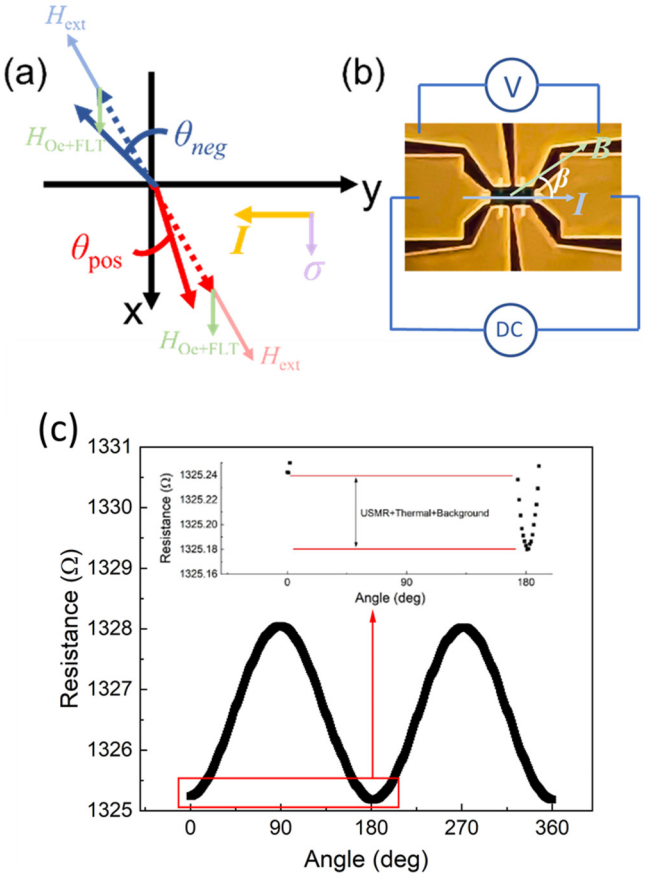

FIG. 1. (a) Illustration of the difference in the magnetization angle under positive and negative fields when a small angular offset of the external field (dashed line is the original offset angle) exists. (b) Illustration of angular-dependent DC measurement setup in Ta/CFB samples. (c) The angular dependence of the Ta/CFB sample. The majority of the signal is AMR, and the inset is a zoom-in view of the signals at 0° and 180°.

Theoretically, the SOT effect cannot result in any difference in magnetization if the magnetization is aligned perfectly perpendicular to the current direction. However, the alignment of the current direction and the field may have a small offset in the experimental setup in field sweep measurements. Few works have looked into this effect and found the value of the potential contribution from AMR to the UMR signal.

A small offset of the external field relative to the x axis is assumed to exist in the measurement setup, the configuration of which is shown in Fig. 1(a). Consider the Ta/CoFeB(CFB) system, where the current flows in y and the spin direction is x. The Oersted field and field-like torque effective field $\mathbf{H}_{Oe+FLT}$ points toward the x-direction no matter what the external field direction is. In this case, the existence of an x-direction field will result in a difference in the angle between the magnetization and x axis when the field is positive and negative, which will then result in an AMR contribution to the total signal of UMR.

To quantitatively study this effect, we deposited a Ta(5)/CoFeB(5)/MgO(2)/Ta(1.5) structure (all thicknesses in nm) and patterned it into a Hall bar structure. A 2 mA DC current is applied to the sample. The field is rotated in-plane, and the DC voltage is measured, as shown in Fig. 1(b). The angular-dependent resistance is shown in Fig. 1(c), which can be fitted using the equation:

$$V_{total} = V_{AMR}\cos(2\beta) + V_{UMR}\cos\beta + C, \quad (1)$$

where AMR gives the major signal with a period of 180°, and UMR (in this case, USMR only) plus thermal effects give the signal with a period of 360°, which is magnitudes smaller than the AMR signal. Note that the FLT and Oersted field can also give a small contribution, but it does not give any value difference at 0° and 180°,[16] thus it can be neglected while fitting the data. The zoom-in lookout for the angular dependence curve is shown in the upper section of Fig. 1(c). Even the "flat bottom" of the AMR curve around 0° and 180° becomes sharp if we zoom into the UMR scale.

With angular-dependent measurement, the 0° and 180° positions are obtained by fitting the AMR curve vs the angle. We now further investigate the Oersted field and FLT-induced SOT contribution. The Oersted field plus the FLT effective field, $\mathbf{H}_{Oe+FLT}$, is obtained by second harmonic measurements in the Ta(5)/CoFeB(5)/capping sample. The obtained values of $\mathbf{H}_{Oe+FLT}$ under different current values are shown in the second row of Table I, while the current values are in the first row. The Ta/CoFeB sample has in-plane anisotropy, which means the anisotropy is easy-plane rather than easy-axis. The coercivity for the in-plane CoFeB is smaller than 30 Oe,[17,18] and the demagnetization field is neglected in our consideration of the angular difference. As there is no easy-axis anisotropy, the CoFeB magnetization direction should be parallel to the total effective field direction.

Now considering an angular offset of the external field, for example, 3°. A small angular change can result in an AMR contribution that has the same magnitude as the difference of a 360° signal at 0° and 180°. However, the existence of the y-direction effective field can result in the magnetization direction slightly off the original offset value and toward different directions at different field directions, as shown in Fig. 1(a). The magnetization is parallel

TABLE I. The values of effective field $\mathbf{H}_{Oe+FLT}$, magnetization offset angle θ_{pos}, θ_{neg}, the difference of AMR resistance $R_{diffAMR}$, and the UMR R_{UMR+}–R_{UMR-} for experimental and large FLT under different current values. The different angles under positive and negative fields lead to different resistance. The effect is negligible with a small FLT but can be considered when the FLT is large.

Current (mA)	0.5	0.8	1	1.2	1.5
Experimental $\mathbf{H}_{Oe+FLT}$ (Oe)	−0.126	−0.168	−0.218	−0.250	−0.307
θ_{pos} (Experimental $\mathbf{H}_{Oe+FLT}$) (deg)	2.992 5	2.990 0	2.987 0	2.985 1	2.981 7
θ_{neg} (Experimental $\mathbf{H}_{Oe+FLT}$) (deg)	3.007 6	3.010 1	3.013 2	3.015 1	3.018 5
$R_{diffAMR}$ (Experimental $\mathbf{H}_{Oe+FLT}$) (deg)	0.000 078	0.000 10	0.000 13	0.000 15	0.000 19
$R_{UMR+} - R_{UMR-}$ (Ω)	0.006 46	0.010 62	0.013 76	0.016 53	0.021 12
θ_{pos} (large $\mathbf{H}_{Oe+FLT}$) (deg)	2.926 5	2.902 5	2.874 5	2.857 1	2.826 4
θ_{neg} (large $\mathbf{H}_{Oe+FLT}$) (deg)	3.077 3	3.104 3	3.136 9	3.158 0	3.196 3
$R_{diffAMR}$ (Large $\mathbf{H}_{Oe+FLT}$) (Ω)	0.000 8	0.001 0	0.001 4	0.001 6	0.001 9

with the total effective field, which is different at positive or negative external fields since the direction of $\mathbf{H}_{Oe+FLT}$ is unchanged while the direction of the external field is reversed. In this case, the angle θ between the magnetization and y axis will have different values at positive and negative fields, as shown in Fig. 1(a). The third (fourth) row of Table I shows the angle θ_{pos} (θ_{neg}) for positive (negative) external fields under different current values, 50 Oe external field, and a 3° angular offset. With the AMR value extracted from the fitting of Fig. 1(c) signal, the $\mathbf{H}_{Oe+FLT}$-induced AMR contribution of the sample is obtained. The differences of resistance $R_{diffAMR}$, which are induced by the differences of θ_{pos} and θ_{neg}, under positive and negative 50 Oe fields with different current values and 3° angular offset, are shown in the fifth row of Table I, and the UMR values (R_{UMR+}–R_{UMR-}, obtained by both DC and AC measurements) in the Ta/CFB system is shown in the sixth row of Table I.

From Table I, the value of $\mathbf{H}_{Oe+FLT}$-induced AMR is negligible compared to the UMR value (0.0251 Ω difference at the positive and negative fields, which is obtained by both DC and second harmonic methods in the latter parts). However, this conclusion is based on the Ta/CFB material system which only has an FLT effective spin Hall angle smaller than ∼0.03.[19,20] Recently, a variety of materials show a relatively large FLT (up to 158 Oe per 10^7 A/cm^2 current density).[18,21,22] In this case, the effective field $\mathbf{H}_{Oe+FLT}$ will be much larger and comparable to the external field. To demonstrate how much influence can a large FLT give on the measurement, we calculated the θ_{pos}, θ_{neg}, and the $R_{diffAMR}$ values with a larger FLT effective spin Hall angle (∼0.3, ten times of experimental $\mathbf{H}_{Oe+FLT}$), as shown in the seventh, eighth, and ninth row of Table I, respectively. The resulting current-dependent measurement value under 50 Oe field and a 3° offset angle, is shown in Fig. 2(a), where the black squares are the UMR data point, the blue line is the proposed measurement value with measured $\mathbf{H}_{Oe+FLT}$ in Ta/CFB sample, and the red line is the calculated measurement value with larger FLT. The larger FLT can induce a ∼7% contribution to the total measured UMR signal under 50 Oe and a 3° offset in DC measurements. Compared to previously reported UMR values measured by DC,[6,8] the contribution of FLT-induced AMR may be smaller, but the effect is still worth noticing when exploring USMR in different material systems. The offset angle dependence and field dependence of the UMR measured value are shown in Figs. 2(b) and 2(c), respectively, where the black line is the UMR value, and the blue (red) lines are the calculated measurement values under small (large) FLT values. The contribution of FLT can be even larger when the offset angle is larger or the external field is smaller. The field-dependent behavior originates from the angular

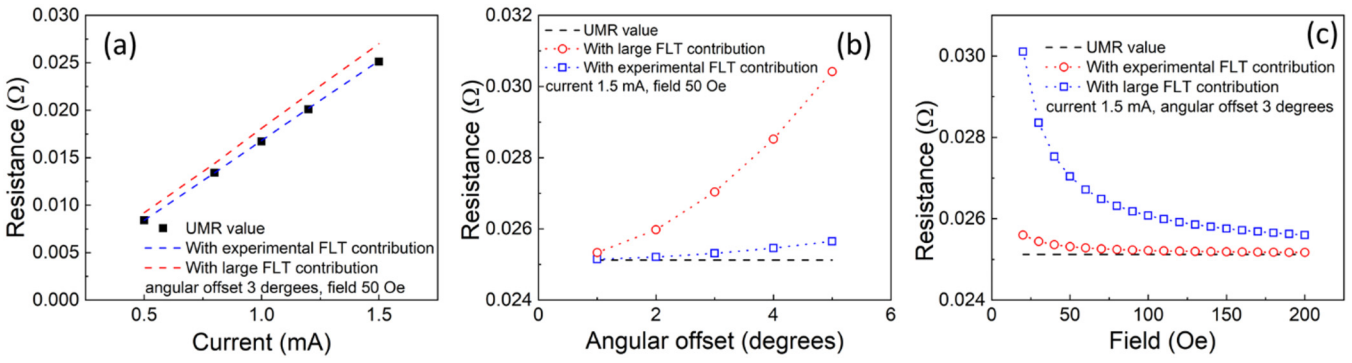

FIG. 2. (a)–(c) Current, angular offset, and field dependence of the measured UMR, respectively. The experimental (small) and large FLT condition is labeled in blue and red, respectively. The black square in (a) and the black line in (b) and (c) represent the UMR value without FLT contributions.

difference of the magnetization at positive or negative fields. In summary, the effect $\mathbf{H}_{\mathrm{Oe+FLT}}$ of is usually negligible but can be a large source of error when a large FLT and an angular offset exist, especially when the external field is small. In this case, the DC method is not a proper method to measure UMR under zero external field if the angular offset cannot be precisely controlled.

B. Influence of the ordinary magnetoresistance

Even without the influence of the SOT effect, obtaining the small UMR value from the field-dependent DC measurement can still be a challenge. The OMR exists in some common SOT material systems,[23,24] and has been a minor effect in SOT measurements and is rarely considered due to its small value. However, this effect can be dominant when measuring a small signal such as UMR. Field-dependent measurements are performed in the Ta/CoFeB sample, as shown in Fig. 3(a). A 1 mA DC current is applied, and the voltage is measured with the Hall bar under different fields. The sample is rotated to a direction without offset using the angular-dependent measurements as shown in Fig. 1(c). The resulting field-dependent resistance curve is shown in Fig. 3(b), where at both positive and negative fields, the resistance decreases when increasing the external field. The increment is quite symmetric under positive and negative fields, suggesting the dominance of OMR.

The OMR signal can be ~1000% of the USMR signal in Ta/CoFeB bilayers, which makes it impossible for DC measurements in such material systems. Even for the observations of large USMR or UMR signals,[6,8] a 0.1 Ω OMR at 2000 Oe can still have an effect of up to 50% of the total signal. It is possible to obtain the UMR value by removing the OMR background. However, the field dependence of OMR is usually not linear,[23,24] especially at low fields, which makes the linear fitting not applicable to obtain the UMR value by interception. Obtaining the different signal at the positive and negative fields at the same field value is a better option. However, the remaining magnetization can always be a problem in the changing field process for magnets, which can result in a different value of the setting and actual field value and result in a larger noise as to our observation. The dominance of OMR means even a small inaccuracy of field value may result in a large signal difference in the measurement.

III. MEASUREMENT METHOD FOR DC UMR

The existence of effective field and OMR has brought challenges to the DC measurement of UMR. An easy-performing standard measurement method is required to obtain an accurate UMR value. This method needs to have the following features: (1) the angular offset must be eliminated to fix the effective field influence. (2) The field value must be accurate at positive and negative values, which could eliminate the OMR contribution. For both features, rotating the sample under a fixed external field is a good solution since the angle can be obtained by fitting, and a fixed field can always be the same at 0° and 180°. Figures 4(a) and 4(b) show the process flow of different contributions in DC UMR measurement. With the field sweep method in Fig. 4(a), the OMR is difficult to remove, and the potential SOT induced AMR contributions can also make signal analysis complex. The angular sweep method in Fig. 4(b) does not contain the OMR and SOT induced AMR contributions, which can directly get the UMR signal by removing AMR background and thermal contributions.

The measurement setup for DC UMR is the same as in Fig. 1(b). Angular sweep measurement is applied to the sample under different fields and currents, and the resulting resistance is obtained using Eq. (1). The term R_{total360} represents the total contributions with a 360° period. The R_{total360} term has multiple contributions: the UMR effect, the thermal effects, and measurement background. The thermal effects include the common anomalous Nernst effect

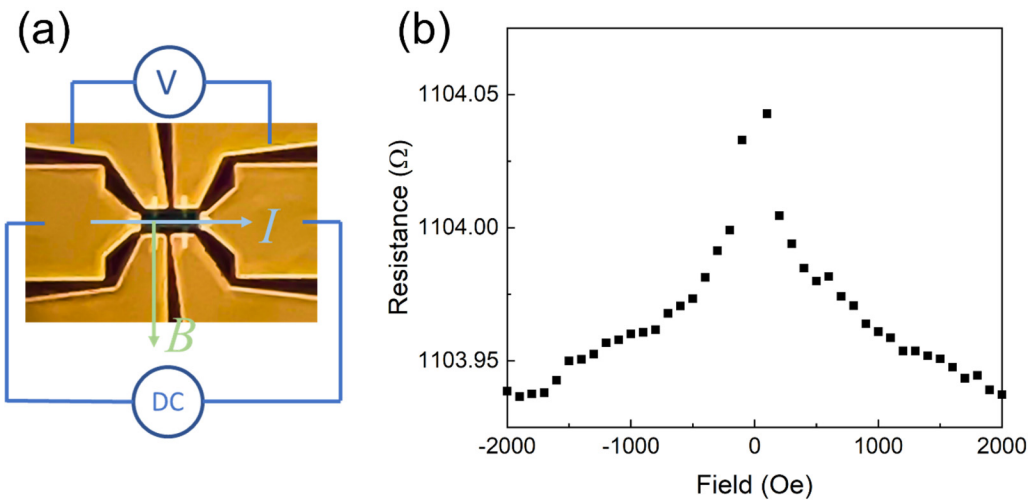

FIG. 3. (a) Illustration of the field-dependent measurement setup with the external field fixed at the x-direction. (b) The field-dependent measurement of the Ta/CoFeB sample shows an OMR background that is comparable to the UMR signal.

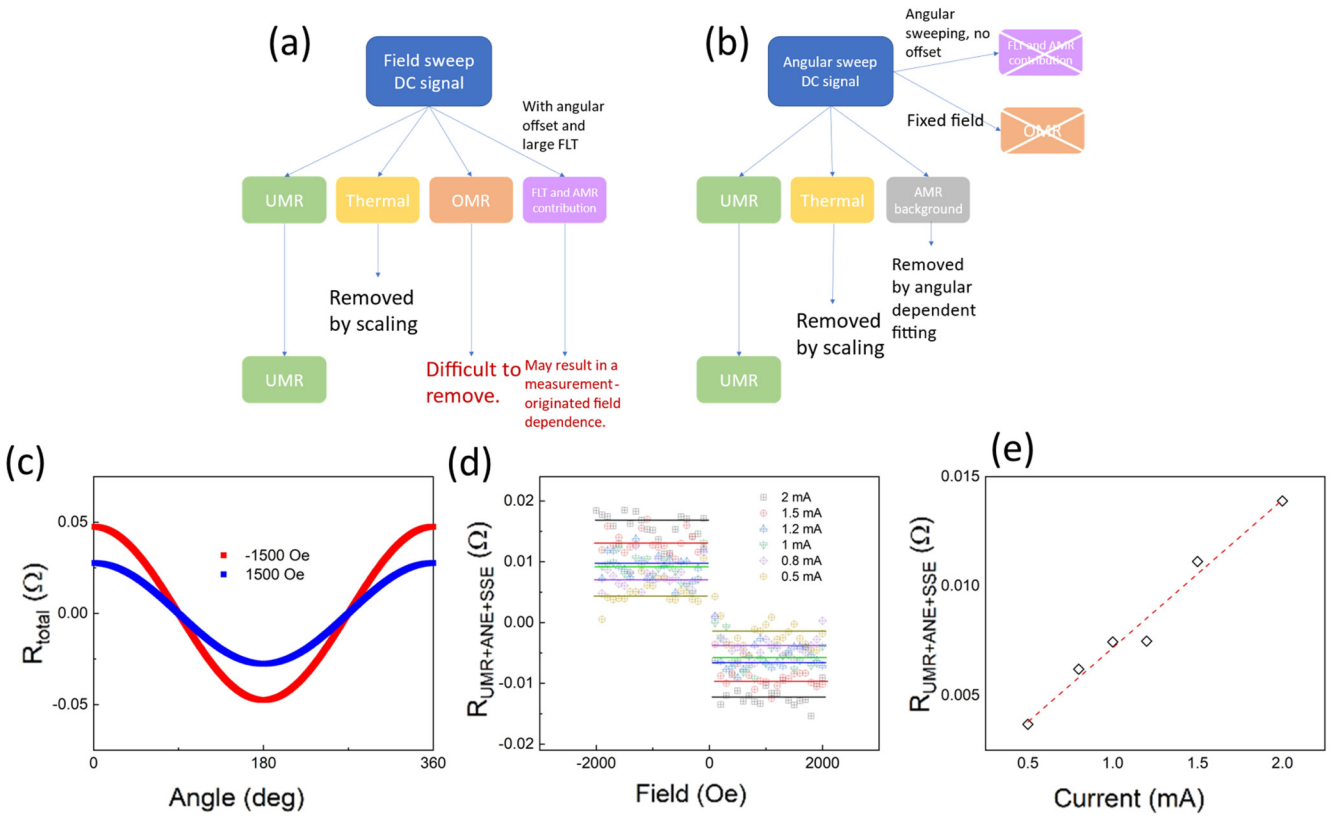

FIG. 4. Process of the signal in (a) field sweep and (b) angular sweep DC UMR measurements. In field sweep measurement, the OMR part is difficult to remove, and the potential SOT induced AMR contributions give rise to the complexity. The angular sweep measurement can avoid OMR and SOT contributions. (c) The fitted value of 360° dependent resistance $R_{total360}$ vs angle at the negative and positive fields. There is a measurement background, and the difference between the positive and negative field fitting is the real contribution of $R_{UMR+ANE+SSE}$. (d) Field dependence of $R_{UMR+ANE+SSE}$ under different current values for the Ta/CFB sample. (e) Plotted $R_{UMR+ANE+SSE}$ vs current shows a linear dependence, which indicates the UMR term in Ta/CFB is dominantly USMR.

(ANE) and spin Seebeck effect (SSE) which are widely studied in SOT measurements and DC UMR measurements.[1–6] In addition, the measurement background exists for the $R_{total360}$ term. Since the measurement background is not dependent on the external field direction and has fixed values, simply sweeping the angle under both positive and negative fields will eliminate this contribution. As shown in Fig. 4(c), the angular dependence of the fitted $R_{total360}$ term (1.5 mA current) has a difference at 1500 and −1500 Oe, and the difference signal can be attributed to the contribution of UMR (in this case, USMR) and field-dependent thermal effects such as ANE and SSE.

With the measurement background contribution removed, the field dependence of $R_{UMR+ANE+SSE}$ can be obtained by fitting different angular-dependent curves under different fields and different current values. With the angular offset removed by angular-dependent fitting, no field dependence will be observed if the system itself does not have field-dependent UMR. The field dependence of $R_{UMR+ANE+SSE}$ under different current values is shown in Fig. 4(d), and the current dependence of $R_{UMR+ANE+SSE}$ is replotted in Fig. 4(e). Both figures show a clear linear dependence of $R_{UMR+ANE+SSE}$ vs the current, which is consistence with the observation of USMR in metallic systems,[1,3,4] and the USMR signal level is repeatable in multiple devices. The obtained value of $R_{UMR+ANE+SSE}$ is ∼0.1 Ω per 10^7 A/cm^2 current density, which is typical for such material systems.[1,3,5–8]

We also performed the well-used second harmonic AC method on the same sample for the validation of the DC method. Since the $R_{UMR+ANE+SSE}$ is proportional to the applied current, the USMR is the only origin of UMR, and the second harmonic method can be accurate to obtain the USMR value. The setup of the AC measurement is shown in Fig. 5(a), where a lock-in amplifier is used to obtain the second harmonic signal. The obtained longitudinal first and second harmonic signals are shown in Fig. 5(b), where the second harmonic signal contains the contributions of USMR, ANE, and SSE, which is similar to the DC measurement case. The values of USMR under different current values are shown in Fig. 5(c). Comparing Figs. 4(e) and 5(c), both DC and AC measurements can obtain the same value of $R_{UMR+ANE+SSE}$. Though the contribution of ANE + SSE cannot be removed in DC measurement, the consistency of DC and AC makes it possible to accurately scale the

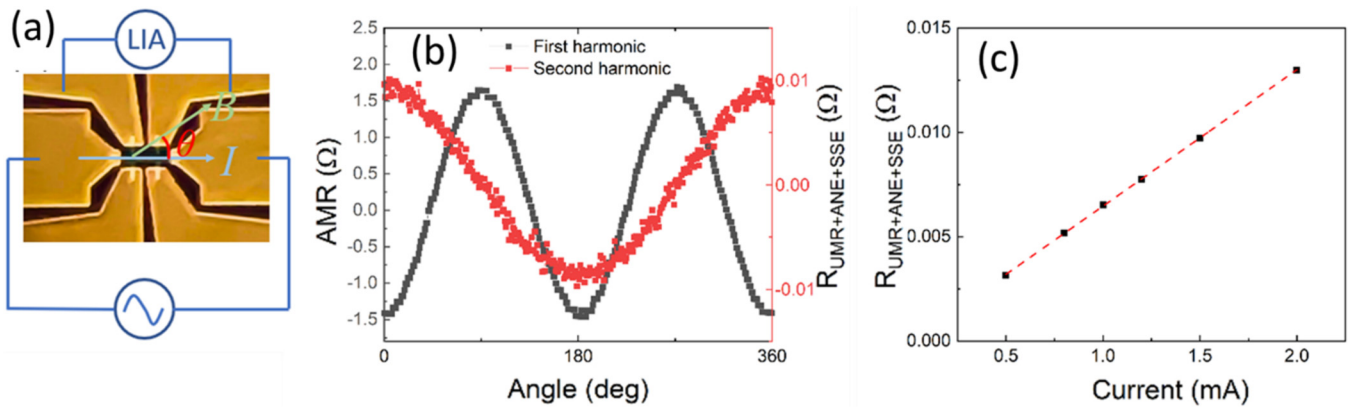

FIG. 5. (a) Illustration of the second harmonic measurement setup. (b) The first harmonic (black) and second harmonic (red) signals represent the AMR and $R_{UMR+ANE+SSE}$, respectively. (c) $R_{UMR+ANE+SSE}$ vs current shows a similar value to Fig. 4(e), suggesting the DC measurement method for UMR is accurate.

DC UMR value by a reference AC measurement.[1,2,7] By measuring the field dependence at Hall direction and geometry scaling,[1–3] the USMR value with thermal contribution is obtained and shown in Fig. 5(c). Since the DC and AC thermal contribution should be identical at low AC frequency, the identical values of total signal in DC and AC measurements suggest a consistency between the two measurement methods.

Compared to the commonly used AC measurement, DC measurement still has limitations such as a small signal-noise ratio, and the incapability to remove the thermal contributions. However, emerging UMR effects with non-quadratic voltage still require an accurate DC measurement. If non-quadratic components exist in the UMR voltage, the demonstrated method can also clearly show it. Though the thermal contributions always exist in the UMR, they can still be scaled using the widely used Hall direction geometry method with second harmonic measurements.[1,2,7] In this case, if AC and DC measurements are combined, the accurate UMR value can still be measured by AC scaling, while the DC measurement can keep the non-quadratic current-dependent features for the UMR signal.

IV. CONCLUSIONS

The emerging observations of different UMR schemes have pushed the application of DC measurement methods in UMR research. Details including the background removal and angular setup are not fully revealed in previous works with DC measurements,[6,8] which makes repeating difficult due to the large observational errors in DC measurements. Compared to AMR and OMR, the small magnitude of UMR can make obtaining real values difficult. This work studied the contribution of FLT in UMR DC measurements and demonstrated how to measure DC UMR accurately. Thermal backgrounds are widely removed in second harmonic measurements but relatively difficult to remove in DC cases. In this study, combining DC and AC measurements were proposed to remove thermal backgrounds with non-quadratic features of UMR revealed in DC measurements. In summary, this work discussed the potential errors in DC measurement for a small signal like UMR and provided a reliable way to observe the existence of UMR via DC measurements.

ACKNOWLEDGMENTS

This work was supported, in part, by SMART, one of the seven centers of nCORE, a Semiconductor Research Corporation Program, sponsored by the National Institute of Standards and Technology (NIST) and by the UMN MRSEC Program under Award No. DMR-2011401. This work utilized the College of Science and Engineering (CSE) Characterization Facility at the University of Minnesota (UMN) supported, in part, by the NSF through the UMN MRSEC program. Portions of this work were conducted in the Minnesota Nano Center, which is supported by the National Science Foundation through the National Nano Coordinated Infrastructure Network (NNCI) under Award No. ECCS-2025124. J.-P.W. also acknowledges support from Robert Hartmann Endowed Chair Professorship.

AUTHOR DECLARATIONS

Conflict of Interest

The authors have no conflicts to disclose.

Author Contributions

Y.F. and J.-P.W. designed the experiments. Y.F. and Y.Y. performed the experiments and wrote the paper with inputs from all authors. R.S. helped with the magnetostatics effort. J.-P.W. secured the funding and coordinated the project.

Yihong Fan: Conceptualization (equal); Data curation (equal); Formal analysis (equal); Methodology (equal); Writing – original draft (equal); Writing – review & editing (equal). **Renata Saha:** Formal analysis (equal); Methodology (equal); Writing – review & editing (equal). **Yifei Yang:** Data curation (equal); Formal analysis (equal); Writing – review & editing (equal). **Jian-Ping Wang:**

Conceptualization (equal); Funding acquisition (equal); Project administration (equal); Supervision (equal).

DATA AVAILABILITY

The data that support the findings of this study are available from the corresponding author upon reasonable request.

REFERENCES

[1]C. O. Avci, K. Garello, A. Ghosh, M. Gabureac, S. F. Alvarado, and P. Gambardella, "Unidirectional spin Hall magnetoresistance in ferromagnet/normal metal bilayers," Nat. Phys. **11**, 570 (2015).

[2]Y. Lv, J. Kally, D. Zhang, J. S. Lee, M. Jamali, N. Samarth, and J.-P. Wang, "Unidirectional spin-Hall and Rashba–Edelstein magnetoresistance in topological insulator-ferromagnet layer heterostructures," Nat. Commun. **9**, 111 (2018).

[3]C. O. Avci, J. Mendil, G. S. Beach, and P. Gambardella, "Origins of the unidirectional spin Hall magnetoresistance in metallic bilayers," Phys. Rev. Lett. **121**, 087207 (2018).

[4]Zhang, S.-L. Steven, and G. Vignale, "Theory of unidirectional spin Hall magnetoresistance in heavy-metal/ferromagnetic-metal bilayers," Phys. Rev. B **94**, 14 (2016).

[5]Y. Yin, D.-S. Han, M. C. d. Jong, R. Lavrijsen, R. A. Duine, H. J. Swagten, and B. Koopmans, "Thickness dependence of unidirectional spin-Hall magnetoresistance in metallic bilayers," Appl. Phys. Lett. **111**, 23 (2017).

[6]D. Khang, N. Huynh, and P. N. Hai, "Giant unidirectional spin Hall magnetoresistance in topological insulator–ferromagnetic semiconductor heterostructures," J. Appl. Phys. **126**, 23 (2019).

[7]Y. Lv, J. Kally, T. Liu, P. Quarterman, T. Pillsbury, B. J. Kirby, A. J. Grutter *et al.*, "Large unidirectional spin Hall and Rashba–Edelstein magnetoresistance in topological insulator/magnetic insulator heterostructures," Appl. Phys. Rev. **9**, 1 (2022).

[8]T.-Y. Chang, C.-L. Cheng, C.-C. Huang, C.-W. Peng, Y.-H. Huang, T.-Y. Chen, Y.-T. Liu, and C.-F. Pai, "Large unidirectional magnetoresistance in metallic heterostructures in the spin transfer torque regime," Phys. Rev. B **104**, 2 (2021).

[9]K.-J. Kim, T. Li, S. Kim, T. Moriyama, T. Koyama, D. Chiba, K.-J. Lee, H.-W. Lee, and T. Ono, "Possible contribution of high-energy magnons to unidirectional magnetoresistance in metallic bilayers," Appl. Phys. Express **12**, 6 (2019).

[10]I. V. Borisenko, V. E. Demidov, S. Urazhdin, A. B. Rinkevich, and S. O. Demokritov, "Relation between unidirectional spin Hall magnetoresistance and spin current-driven magnon generation," Appl. Phys. Lett. **113**, 062403 (2018).

[11]W. P. Sterk, D. Peerlings, and R. A. Duine, "Magnon contribution to unidirectional spin Hall magnetoresistance in ferromagnetic-insulator/heavy-metal bilayers," Phys. Rev. B **99**, 064438 (2019).

[12]G. Liu, X.-g. Wang, Z. Z. Luan, L. F. Zhou, S. Y. Xia, B. Yang, Y. Z. Tian, G.-h. Guo, J. Du, and D. Wu, "Magnonic unidirectional spin Hall magnetoresistance in a heavy-metal–ferromagnetic-insulator bilayer," Phys. Rev. Lett. **127**, 20 (2021).

[13]M. Hayashi, J. Kim, M. Yamanouchi, and H. Ohno, "Quantitative characterization of the spin-orbit torque using harmonic Hall voltage measurements," Phys. Rev. B **89**, 144425 (2014).

[14]X. Qiu, Z. Shi, W. Fan, S. Zhou, and H. Yang, "Characterization and manipulation of spin orbit torque in magnetic heterostructures," Adv. Mater. **30**, 17 (2018).

[15]M. Dc, R. Grassi, J.-Y. Chen, M. Jamali, D. R. Hickey, D. Zhang, Z. Zhao *et al.*, "Room-temperature high spin–orbit torque due to quantum confinement in sputtered BixSe (1–x) films," Nat. Mater. **17**, 9 (2018).

[16]X. Fan, J. Wu, Y. Chen, M. J. Jerry, H. Zhang, and J. Q. Xiao, "Observation of the nonlocal spin-orbital effective field," Nat. Commun. **4**, 1 (2013).

[17]L. Kipgen, H. Fulara, M. Raju, and S. Chaudhary, "In-plane magnetic anisotropy and coercive field dependence upon thickness of CoFeB," J. Magn. Magn. Mater. **324**, 3118 (2012).

[18]Y. Fan, H. Li, M. Dc, T. Peterson, J. Held, P. Sahu, J. Chen, D. Zhang, A. Mkhoyan, and J.-P. Wang, "Spin pumping and large field-like torque at room temperature in sputtered amorphous WTe_{2-x} films," APL Mater. **8**, 4 (2020).

[19]K. Garello, I. M. Miron, C. O. Avci, F. Freimuth, Y. Mokrousov, S. Blügel, S. Auffret, O. Boulle, G. Gaudin, and P. Gambardella, "Symmetry and magnitude of spin–orbit torques in ferromagnetic heterostructures," Nat. Nanotechnol. **8**, 587 (2013).

[20]C. Zhang, M. Yamanouchi, H. Sato, S. Fukami, S. Ikeda, F. Matsukura, and H. Ohno, "Magnetotransport measurements of current induced effective fields in Ta/CoFeB/MgO," Appl. Phys. Lett. **103**, 26 (2013).

[21]K. Kondou, H. Chen, T. Tomita, M. Ikhlas, T. Higo, A. H. MacDonald, S. Nakatsuji, and Y. Otani, "Giant field-like torque by the out-of-plane magnetic spin Hall effect in a topological antiferromagnet," Nat. Commun. **12**, 6491 (2021).

[22]S. Dutta, A. Bose, A. A. Tulapurkar, R. A. Buhrman, and D. C. Ralph, "Interfacial and bulk spin Hall contributions to fieldlike spin-orbit torque generated by iridium," Phys. Rev. B **103**, 18 (2021).

[23]L. Shen, D. S. Schreiber, and A. J. Arko, "Magnetoresistivity of a dilute Pt:(Co) alloy," J. Appl. Phys. **40**, 3 (1969).

[24]L. Baldrati, A. Ross, T. Niizeki, C. Schneider, R. Ramos, J. Cramer, O. Gomonay *et al.*, "Full angular dependence of the spin Hall and ordinary magnetoresistance in epitaxial antiferromagnetic NiO (001)/Pt thin films," Phys. Rev. B **98**, 2 (2018).